5-9-2020

Dynamic Characterization of DuroProtect, a Fiber-Reinforced Ballistics Composite

Ivy A. Turner

Follow this and additional works at: https://egrove.olemiss.edu/hon_thesis

Part of the Acoustics, Dynamics, and Controls Commons, and the Other Materials Science and Engineering Commons

DYNAMIC CHARACTERIZATION OF DUROPROTECT, A FIBER-REINFORCED BALLISTICS COMPOSITE

By

Ivy Alaysa Turner

A thesis submitted to the faculty of The University of Mississippi in partial fulfillment of the requirements of the Sally McDonnel Barksdale Honors College.

Oxford

May 2020

Approved by

_____

Advisor: Mr. Damian Stoddard

_____

Reader: Dr. A. M. Rajendran

_____

Reader: Dr. Tejas Pandya

ii

ACKNOWLEDGEMENTS

ABSTRACT

IVY ALAYSA TURNER: Dynamic Characterization of Duroprotect, A Fiber-Reinforced
Composite

Dynamic characterization of materials has become increasingly common, as it is important
to understand how materials behave under sudden loads. Understanding these properties can aid in
material selection for novel designs. DuroProtect, a fiber-reinforced ballistics composite developed
by Röchling, was tested for its dynamic properties at high strain-rates. The Split Hopkinson
Pressure Bar (SHPB) test was used to obtain dynamic properties at high strain-rates under
compressive loading conditions. Tests were initially conducted to validate force equilibriums for
each sample. The data measured from the strain gages mounted on the incident and transmission
bars and the elastic wave propagation theories yields the stress-strain curves. DuroProtect Level 1
and Level 2 samples were tested at strain rate ranges between ~800/s to ~1900/s and ~1300/s to
~2000/s, respectively. Differences between Level 1 and Level 2 samples were attributed by the
number of fiber layers and thickness of the manufactured panels. Results showed no conclusive
evidence for strain-rate sensitivity within the strain-rates tested for Level 1 or Level 2, as initially
hypothesized. A comparison study between the two thicknesses revealed that Level 1 had the
greatest ultimate compressive strength at a range of 547-595 MPa. Level 2, however, had the
greatest specific energy of 25-44 kJ. The Level 1 and Level 2 stress-strain measurements for the
DuroProtect composite were consistent with the properties expected for fiber-reinforced
composites, although there is no conclusive evidence of strain-rate sensitive behaviors within the
tested ranges of strain-rates.

TABLE OF CONTENTS

LIST OF FIGURES

LIST OF EQUATIONS

LIST OF ABBREVIATIONS

SHPB .... Split Hopkinson Pressure Bar

DIC... Digital Image Correlation

IED...Improvised Explosive Devices

GUI .... Graphical User Interface

INTRODUCTION

Purpose

Although composites have existed for millennia as cellulose, they have become more complex in the recent years. Engineers have successfully used a variety of composites, especially fiber-based composites in several structural applications for nearly a century [1]. Composites take the best or desired properties of various homogenous materials and combine them into a superior material. Composites are generally constructed to make designs lightweight but durable and strong. Composites have shown great promise in several fields of design. Hypercars have been utilizing carbon fiber composites as its entire body structure to emphasize power over weight. Aircraft support structures were once made with wood and aluminum skins to be lightweight for flight. Composites are also utilized in building materials, most commonly concrete. Whichever the sort, composites are becoming widely used; however, their behaviors under dynamic loading conditions are still not fully understood due to anisotropy and heterogeneities.

Standard tests performed on novel materials are often quasistatic, simulating still, constant loading conditions at strain rates less than 1 /s. These quasistatic experiments are usually tensile, compressive, flexural, or torsional in nature. For the past five decades, several test methods, such as the SHPB test, low velocity impact test, and shock tube test, had been developed towards obtaining properties under dynamic loading conditions. The SHPB is one of the most utilized testing methods which provide vital measurements. Dynamic loading tests in the form of impact and vibration have shown that materials can behave differently as compared to quasistatic tests. In the present work, the compression SHPB apparatus is employed to determine the stress-strain curves for two types of composite material systems. Since collision between two solids generate extreme compressive loadings under very high strain rates, it is important to subject the experimental samples under similar loading conditions to obtain meaningful results. A stress vs. strain curve for the composite material can be determined using data from the strain gauges

mounted on the incident and transmission bars in the SHPB experiment. In the data reduction scheme, the equations related to elastic wave propagations in bars under uniaxial stress conditions are employed. The stress vs. strain curves at different strain-rates provide several key properties, such as energy absorption, strain-to-failure, and compressive strength.

DuroProtect is manufactured by Röchling as part of their ballistic composite series. Consisting of layered 90-90 fiber weave and a resin matrix, the ballistics panels can have multiple uses. With possible benefits in military, construction, and automotive applications, it can be a revolutionary material that saves in weight and cost compared to conventional ballistic materials. In addition to being certified for several ballistic standards on large-caliber small arms, such as UL-752, EN 1522/1523, and VPAM PM2007, it also can serve as protection against large-scale blasts and impacts from improvised explosive devices (IEDs) and shrapnel. Due to these properties, its most popular use is as a lining material for safe houses. It is also flame retardant and relatively easy to machine [2].

Compressive strength of most materials such as metals, ceramics, cement, rocks, and some composites increase with increasing strain rate. This behavior is often called as strain rate dependent or sensitive behavior of materials. The main purpose of this experiment was to measure dynamic properties of DuroProtect as well as to determine whether it is subject to strain-rate sensitivity in a range of high strain rates. A comparison of the dynamic response between Level 1 and Level 2 panel thicknesses was also constructed. Data determined from this research can be logged as a resource under a material database and such data will be very useful in car crash worthiness design analysis.

Dynamic Testing

Based on previous studies, materials can exhibit different engineering properties based upon the duration and amount of loading. Materials are typically characterized by their strength

properties under quasi-static loading conditions, but dynamic loading should also be considered when applicable. Common examples of dynamic loading could be a sudden impact by an explosion, crash, or fall. Testing how a material reacts under dynamic loading conditions increases knowledge about its limits and helps to inform decisions during material selection, as well as design for more impact-resistant systems. There are several ways to test materials under dynamic loading conditions. The Split Hopkinson Pressure Bar Test (SHPB) simulates a dynamic load, or rather a high strain-rate loading scenario. In this experiment, the SHPB method was used to understand the dynamic properties of DuroProtect, a fiber-reinforced ballistics composite panel. Low-velocity impact is another test utilized to identify any dynamic material properties. In this test, a punch is accelerated into a sample, shearing through the sample's thickness. Another test to consider requires the use of a shock tube. Intense amounts of pressure builds up behind several sets of diaphragms to simulate very high strain-rate scenarios.

Background research

Compared to previous studies on other fiber composite materials, DuroProtect was expected to exhibit similar properties. It was also expected to show strain-rate sensitivity at high strain-rates. Several studies suggested a strain-hardening effect in their respective fiber reinforced composites. The SHPB method was utilized to conduct high strain-rate loading tests on the DuroProtect samples as other studies.

A study by Omar, et al. explored the dynamic properties of natural fiber composite materials made with 7:3 ratios of jute or kenaf fibers to unsaturated polyester. Experiments compared dynamic properties of samples tested under quasi-static loading and a range of high strain-rate loading from ~1020/s to ~1340/s. Not only were there significant increases in ultimate compressive strength found with the SHPB method compared to quasi-static testing, but also a strain hardening dependence was observed. Quasi-static loading at 0.001/s yielded a maximum compressive strength of 75.3 MPa for jute fiber reinforced composites. Kenaf fiber reinforced

composites had a maximum compressive strength of 45.8 MPa. A strain-rate of 1340/s was achieved on the SHPB apparatus, and the maximum compressive strengths obtained were 150.6 MPa and 87.6 MPa for jute and kenaf fiber composites respectively [3].

A similar study by Guden, Yildirin, and Hall showed dynamic characteristics through the SHPB method of plain-weave S-2 fiber layers with a SC-15 epoxy matrix. Similar to DuroProtect, the layers were normal to the thickness and was used as a backing plate for composite armor. Tested strain-rates ranged from 0.0001/s to 1100/s. Maximum compressive stress increased from 450 MPa to 700 MPa as strain-rate increased. Thus, the strain-hardening effect was identified. Failure was mostly attributed to matrix cracking at interlaminar boundaries [4].

Yet another study by Naik et al. utilized the SHPB apparatus to test 40% woven E-glass to 60% epoxy. The study focused on the tensile behavior of the fiber composite along the thickness, warp, and fill directions with strain-rates ranging from ~140/s to 400/s. Tensile strength increased by 11% in the thickness direction as strain-rate increased. Again, the strain hardening effect was observed and concluded to be attributed to the little time allowance for damage propagation at microcracks and defects in the samples [5].

Several thermoset and thermoplastic fiber composites used in the automotive industry have been dynamically tested by Kim et al. Various ratios and combinations of natural hemp, wheat straw, cellulose, and glass fibers were dynamically tested under the SHPB method at strain-rates from ~600/s to ~2400/s. Results found definite strain-hardening effects in each sample category. Maximum stress for samples tested between ~1500/s to ~2300/s ranged between 219 MPa to 309 MPa [6].

Hypothesis

Based upon previous studies, DuroProtect was believed to share similar results with other fiber-reinforced materials. All fiber-reinforced samples observed had higher stress values with

increasing strain-rates from quasistatic to dynamic rates. The general trend of increasing maximum stress values with increasing strain rates was expected, thus assuming the DuroProtect samples for both Level 1 and Level 2 would have exhibited strain rate sensitivity and a strain hardening effect within the tested range.

MATERIALS AND METHODS

DuroProtect

The DuroProtect samples were manufactured and developed by Röchling, a multi-divisional plastics company. The samples provided were from the Glastic Composite Division as a product of their ballistic composite series. Two 1ft x 1ft panel samples were comprised of 90-90 woven, fibrous sheets layered within a sort of resin matrix. Actual ingredients were not provided, as the makeup of the product is proprietary information. The two panels were manufactured in different thicknesses, denoted by Level 1 and Level 2. Level 1 had an average thickness of 7.5 mm, while Level 2 had an average thickness of 8.25 mm. These panels had to be cut down into smaller samples that would fit within the diameter of bars in the SHPB setup. A 1:1:1 aspect ratio for the length, width, and height of each sample was maintained, as per recommendation by accepted suggestions for the SHPB method [7]. Samples were cut on a vertical band saw with a diamond-impregnated blade, suggested by the manufacturer, in the department machine shop. Water lubrication was not used in order to maintain the integrity of each sample by avoiding the introduction of foreign substances that could potentially skew results. Studies by Zivkovic et al. and Barbosa et al. showed increases in mechanical properties of fiber composite samples exposed to accelerated aging by moist environments [8] [9]. A respirator was required during the cutting process for health and safety. Figure 1 shows cut samples of Level 2 DuroProtect.

Figure 1: Level 2 DuroProtect Samples

Elastic Wave Theory

The SHPB method is contingent upon force equilibrium. The elastic wave theory demonstrates how stress in the sample is determined from strain measured in the bars. A stress wave is formed as an incident wave and travels through the bars, with the sample in between the incident bar and transmitted bar. As the wave passes through, the bars are displaced and temporarily deformed. Strain gages adhered to the bars quantify strain in the bars. Strain is the change in length of the sample over the original length of the sample, as denoted by Equation 1.

$$\varepsilon = \frac{\delta}{l_0} \quad \text{(Equation 1)}$$

where ε is strain, δ is change in length [m], and l_0 is original length [m] [10].

The displacement of the bars is first determined. Equations 2 and 3 are the displacements for the incident bar and transmitted bar, respectively.

$$\delta_1 = \int_0^t C_o \varepsilon_1 dt \quad \text{(Equation 2)}$$

$$\delta_2 = \int_0^t C_o \varepsilon_2 dt \quad \text{(Equation 3)}$$

where U_1 and U_2 are the displacements of the incident bar and transmitted bar respectively, t is time [s], C_0 is the wave speed within the bar [m/s], and ε_1 and ε_2 are the strains in the incident bar and transmitted bar respectively [7].

A portion of the wave passes through the sample as a transmitted wave, while rest is reflected back into the incident bar as a reflected wave. Figure 2 shows the general trend of the three waves measured in the bars as the stress wave passed through the sample.
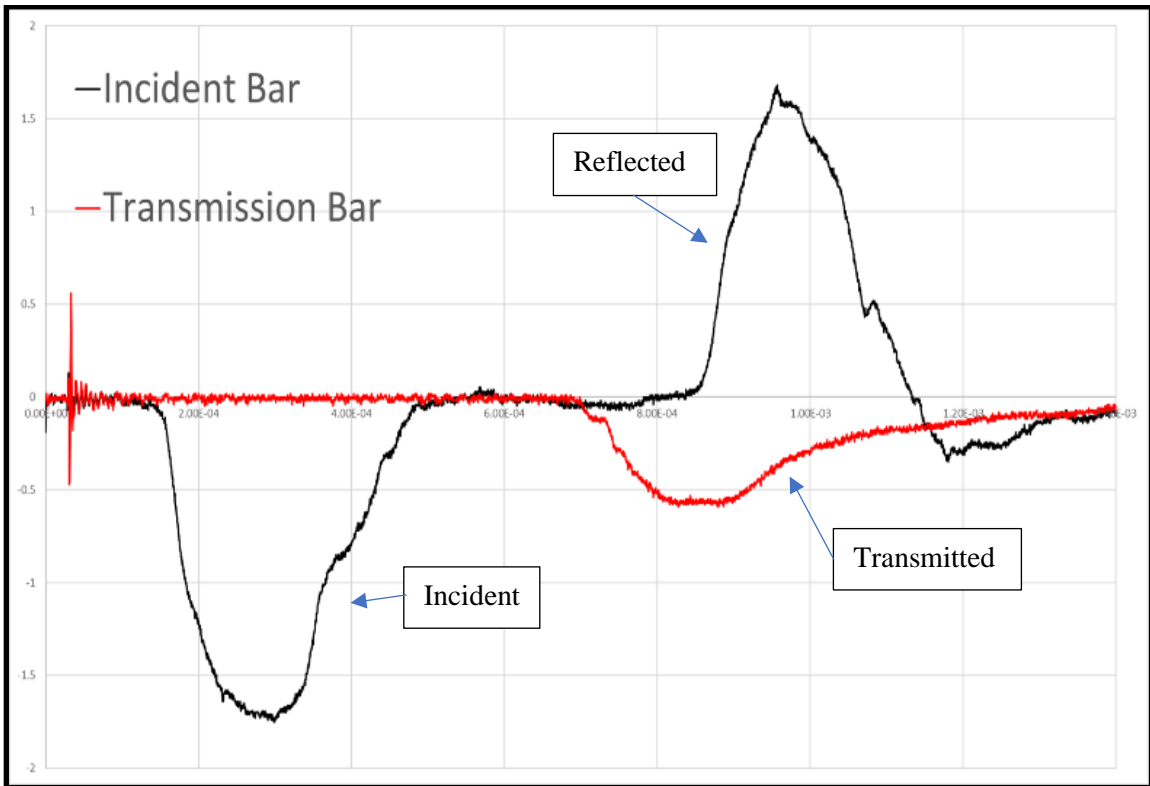
Figure 2: General diagram of Incident, Transmitted, and Reflected waves

By convention, compressive forces are negative, as the current length of the sample becomes smaller than the original sample. However, since the impact forces in this test are always compressive, the compressive strain is considered positive in the compressive direction, while tensile strain is considered negative in the compressive direction. Equations 4 and 5 are constructed based upon this observation.

$$\varepsilon_1 = \varepsilon_i - \varepsilon_r \quad \text{(Equation 4)}$$

$$\varepsilon_2 = \varepsilon_t \quad \text{(Equation 5)}$$

Where ε_i is the strain due to the initial incident wave, ε_r is the strain due to the reflective wave (negative due to its opposite motion of initial incident wave), and ε_t is the strain due to the transmitted wave [7].

With this observation, equations 2 and 3 can be rewritten as Equations 6 and 7 [7]:

$$\delta_1 = \int_0^t C_o(\varepsilon_i - \varepsilon_r)dt \quad \text{(Equation 6)}$$

$$\delta_2 = \int_0^t C_o\varepsilon_t dt \quad \text{(Equation 7)}$$

Strain in the sample can now be found by utilizing Equation 1 and the displacements of the incident and transmitted bars in Equation 8.

$$\varepsilon_s = \frac{\delta_1 - \delta_2}{L_o} = \frac{C_o}{l_o}\int_0^t(\varepsilon_i - \varepsilon_r - \varepsilon_t)dt \quad \text{(Equation 8)}$$

Where L_o is the original length of the sample [7].

Maintaining force equilibrium, the sum of the incident and the reflected wave will ultimately equal the transmitted wave. Force equilibrium equations for both the incident and transmitted bar are given as Equations 9 and 10:

$$P_1 = E_1A_1(\varepsilon_i + \varepsilon_r) \quad \text{(Equation 9)}$$

$$P_2 = E_2A_2(\varepsilon_t) \quad \text{(Equation 10)}$$

Where P_1 and P_2 are the forces [N], E_1 and E_2 are the Young's moduli [Pa], and A_1 and A_2 are the cross-sectional areas [m^2], all of the incident and transmitted bar respectively [7].

Following Conservation of Momentum, Equation 11 is constructed.

$$P_1 = P_2 \quad \text{(Equation 11)}$$

9

Assuming the entire bar setup as a singular system with both incident and transmitter bars being of the same material and cross-sectional area as per method requires, Equation 12 is justified.

$$\varepsilon_i + \varepsilon_r = \varepsilon_t \quad \text{(Equation 12)}$$

where ε_i is the strain measured in the incident bar, ε_r is the measured strain that was reflected from the sample, and ε_t is the strain measured in the transmitted bar [7].

The strain in the sample denoted by Equation 8 can now be rewritten as Equation 13:

$$\varepsilon_s = \frac{-2C_o}{L} \int_0^t \varepsilon_r dt \quad \text{(Equation 13)}$$

Where ε_s is the strain in the sample, C_o is the elastic wave speed of the bar, L is the thickness of the sample, and t is time [7].

Stress and strain are linearly related in the elastic region of deformation. The strain within the long bars are very minimal, so the bars' deformation during the test stays within the elastic region. The relation is given by Equation 14:

$$\sigma = E\varepsilon \quad \text{(Equation 14)}$$

Where σ is stress [Pa], E is Young's modulus [Pa], and ε is strain [10].

With the relation in equation 14, the stress in the sample can then be calculated from the given strain by Equation 15. Equation 15 assumes a material impedance and corrects for the cross-sectional area change between the sample and the bar.

$$\sigma_s = E_{bar} \frac{A_{bar}}{A_s} \varepsilon_t \quad \text{(Equation 15)}$$

Where σ_s is the stress in the sample [Pa], E_{bar} is the elastic modulus of the Hopkinson bar [Pa], A_{bar} is the cross-sectional area of the bar [m²], and A_s is the area transverse to the thickness (cross-sectional area)[m²] [7].

Equation 16 gives the strain-rate, or how fast the sample is loaded [7].

$$\dot{\varepsilon}_s = \frac{-2C_o}{L} \varepsilon_r \quad \text{(Equation 16)}$$

EXPERIMENTAL SETUP

Split Hopkinson Pressure Bar Method

SHPB method currently does not have any official testing standards; however, all theory and procedures were followed as outlined per W. Chen and B. Song [7]. The dynamic testing chosen for DuroProtect was the SHPB method in compression. The University of Mississippi is one of the few academic institutions to have the SHPB setup in both tension and compression, low-velocity impact, and a shock tube. The baseline of the setup is outlined in Chen's and Song's Kolsky bar design [7]. All bars are made of maraging steel, with a diameter of 19.05 mm. The striker bar is inserted into the gas gun and is propelled into the incident bar. A copper pulse shaper is placed between the striker bar and incident bar. The material impedance between the maraging steel and ductile copper allowed the stress wave to gradually ramp up to its peak. Without the pulse shaper, the stress wave would enter the sample as a square pulse, forcing all the energy from the impact into the sample instantaneously. This would cause premature failure of the sample, as the stress distribution is unbalanced with a strain rate that is not constant as the wave passes through the thickness of the sample [12] [13]. The incident bar has the first strain gage attached to it, which measures the incident and reflected wave. The sample is placed between the incident and transmission bars. The transmission bar has the second strain gage that measures the transmitted wave after passing through the sample. The momentum trap bar takes the transmitted wave after it has passed through the transmission bar by being displaced away from the transmission bar. Once the stress wave hits the end of the momentum trap bar, it can no longer reflect back into the transmission bar, leaving clean data at the transmission bar's strain gage. Figure 3 is a schematic of the SHPB setup.
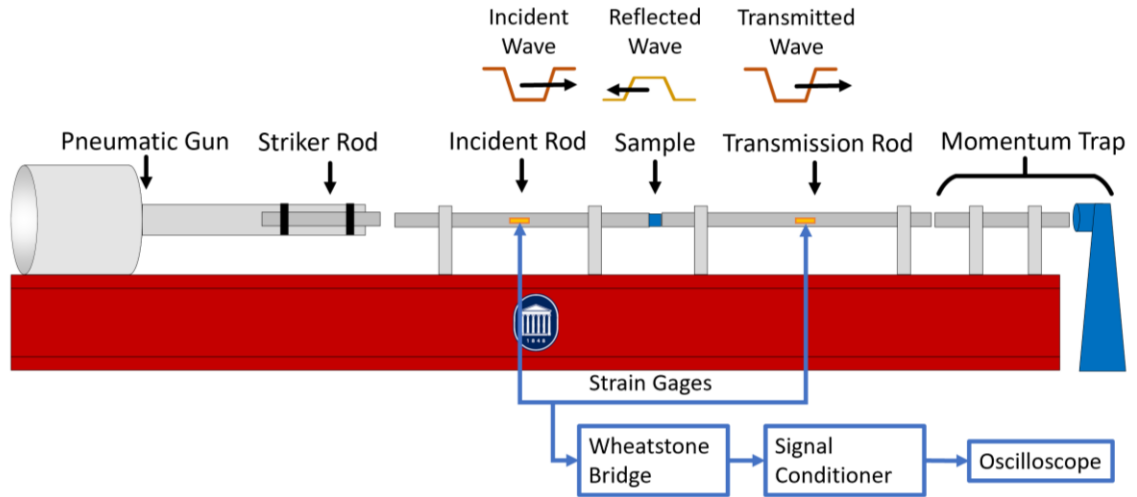
Figure 3: SHPB setup schematic [14]

Each strain gage is attached to an arm of a Wheatstone Bridge set up in quarter bridge configuration with a 5-volt input. A Wheatstone Bridge is a useful circuit that is able to translate the change seen in the resistivity when the strain gage is elongated or compressed. When the strain gage is unchanged from its original length, the bridge is balanced and will have a voltage readout of 0 volts. Any changes in the resistivity of the strain gage will cause an imbalance of the bridge and produce a nonzero voltage output. Two strain gages on each bar are actually used, placed 180 degrees from each other on the bar. This eliminated any strain due to bending. Figure 4 is the Wheatstone Bridge configuration used during this experiment.
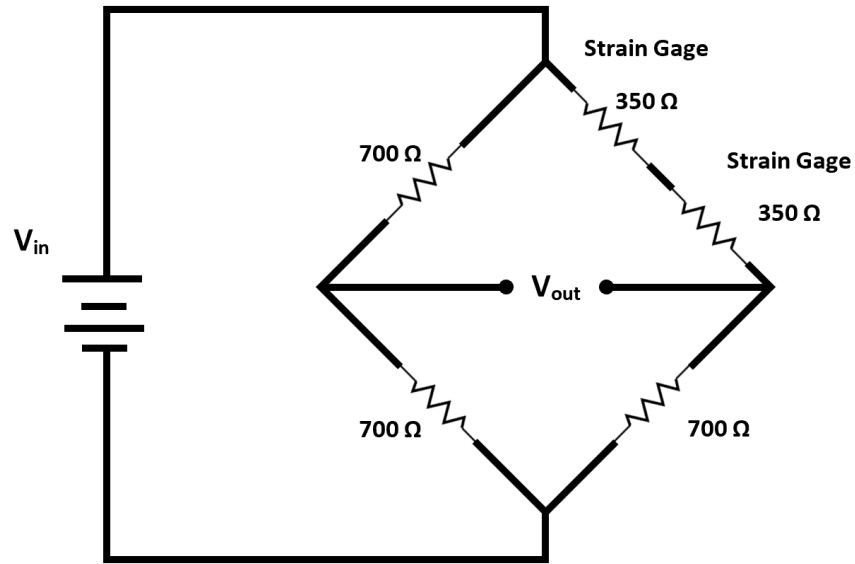
Figure 4: Wheatstone Bridge configuration for SHPB

Collected strain data from Wheatstone Bridge is recorded by a Data Acquisition System. This data is used for strain gage analysis with a MATLAB script. Digital Imaging Correlation (DIC) analysis is also performed in order to compare and ensure strain gage data is valid. A Shimadzu HPV video camera with a camera resolution of 312 x 260 pixels is utilized to take high speed videos. Camera settings are 250,000 frames per second with a recording time of 400 μs. The videos are analyzed with ProAnalyst software to visually capture sample strain. Figure 5 shows the SHPB and DIC setup at the sample placement location.

Figure 5: SHPB and High-Speed Video Setup

Strain Gage Analysis

After testing is completed on all samples, saved strain gage data is uploaded to a computer with MATLAB capabilities. A MATLAB script complete with a Graphical User Interface (GUI) is utilized to analyze the data. Files from the data acquisition is parsed into two .csv files: one for the incident bar and one for the transmission bar. These files are uploaded to the GUI once the code is run. From here, the properties of the bars used are input and the data is shifted accordingly. The strain curves are overlaid onto a single graph. The waves were shifted until force equilibrium is achieved. Figure 6 shows the GUI window with shifted data.
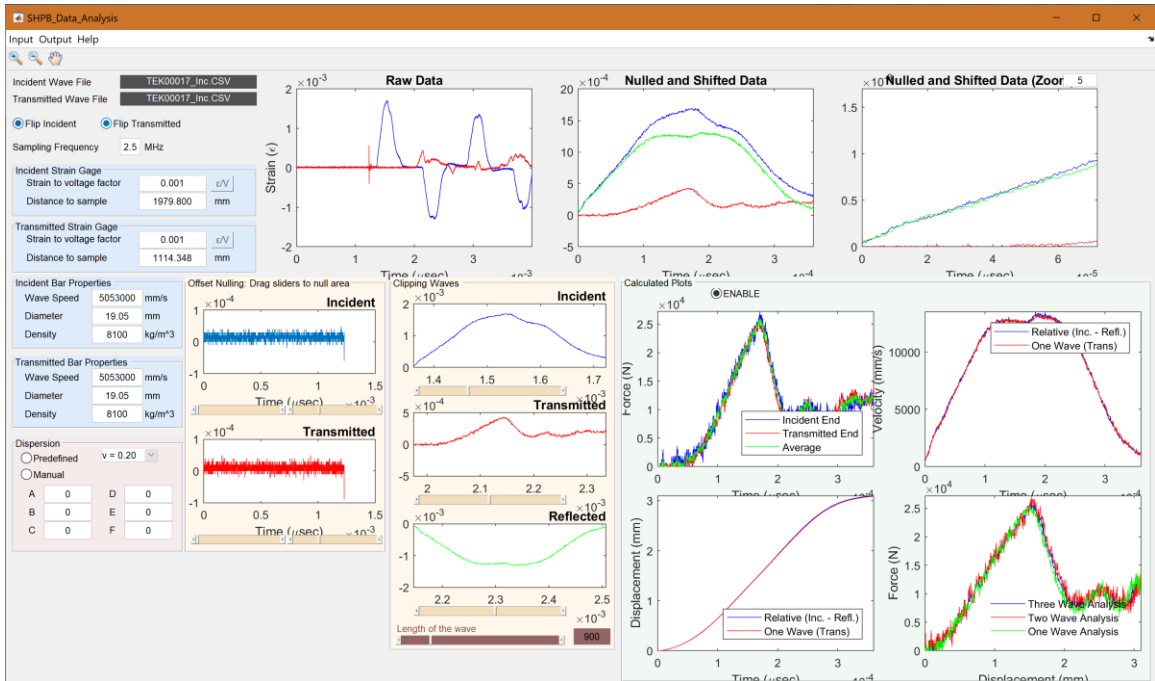
Figure 6: SHPB Data Analysis GUI

Force equilibrium is achieved when the incident end and transmitted end have matching waves. Force equilibrium is also clear with the matching of one, two, and three wave analysis. From here, the data is exported to stress-strain analysis. From the given strain data and dimensions of the sample, the stress is calculated and the script generates a stress vs. strain curve. Figure 7 is the GUI window for stress-strain analysis.
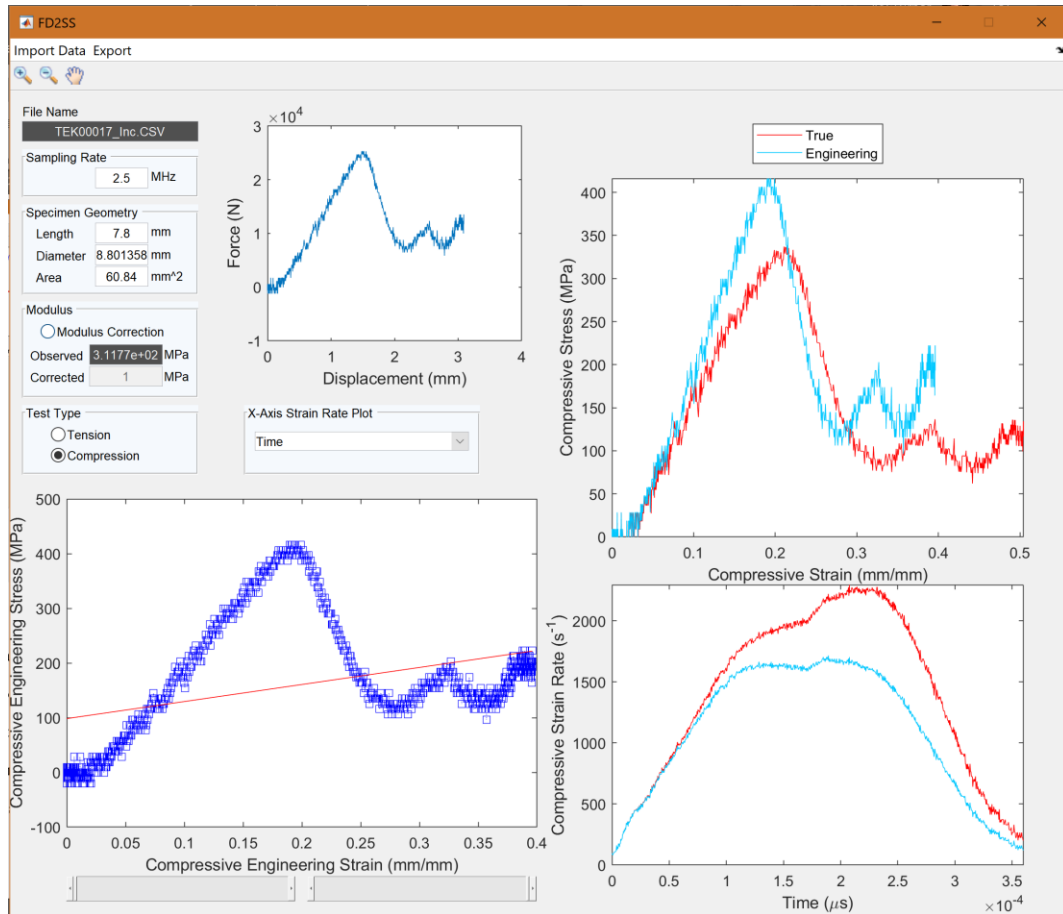
15

Figure 7: Stress-Strain Analysis

This data is then imported into an excel file template with formulas to identify other material properties from the generated stress vs. strain curves. From the Excel file, specific energy, maximum energy, damage initiation energy, damage propagation energy, peak stress, and strain rate are determined. Figure 8 contains several graphs that parse the stress and strain data into meaningful information within Excel.
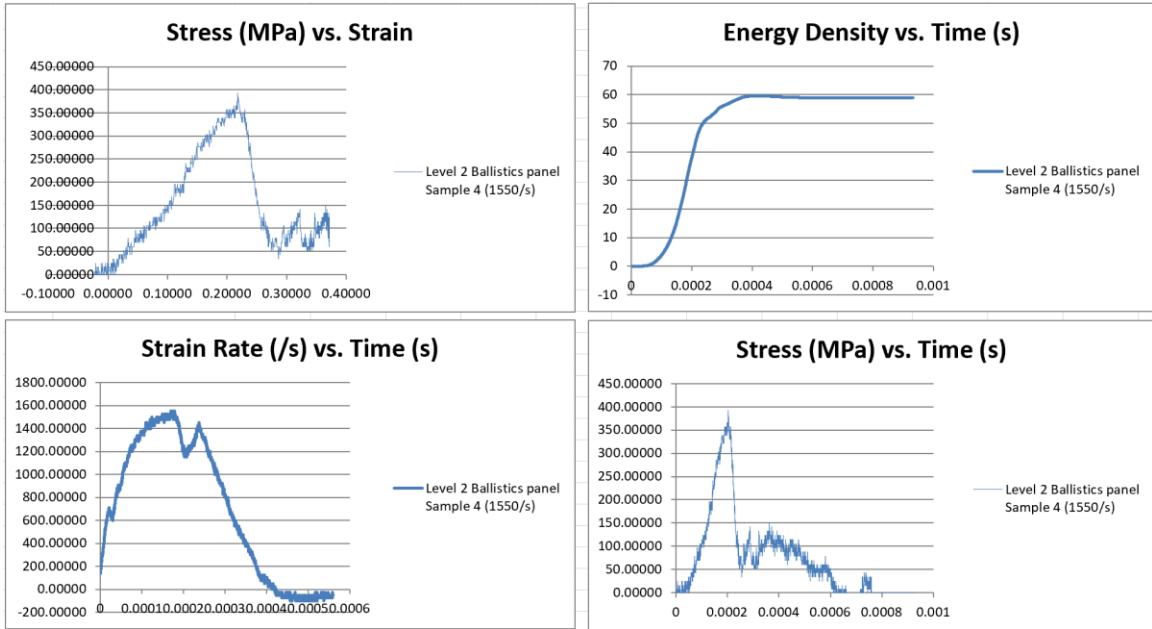
Figure 8: Excel Stress-strain analysis

The stress vs. strain curves give vital information for the dynamic properties. The stress vs. strain curves for each sample can also be overlapped in order to determine any trends.

Digital Image Correlation (DIC) Analysis

Another analysis was also performed during the experiment. DIC used the high-speed videos recorded for each of the samples. DIC tracks individual pixels for each frame of the video capture. It correlates the movement of the pixels and the original length of the sample to determine the strain of the sample at that point in time. It is potentially more accurate than strain gage analysis, since it eliminates any noise in the signal. It is also a useful tool to visually represent stress as it propagates through the sample over time.

The high-speed videos captured 400 μs of the sample failure. This was enough time to view the initial impact and the sample failure, as well as some residual compression after failure. The videos were uploaded to the ProAnalyst software. From here, 1-D motion tracking was started, and the length between the incident and transmission bars, essentially the thickness of the sample, was

measured for each frame of the video. Relating this process to strain, as given by $\varepsilon = \frac{\delta}{l_0}$ (Equation 1), The original length l_0 is the original thickness of the sample. The change in length, δ, is determined by the distance between the two pixels on the moving bars being tracked. The first sight of damage is the point at which the sample fails. The strain was determined at this point, as well as the peak stress. Figure 9 shows the 1-D tracking for a DuroProtect sample.
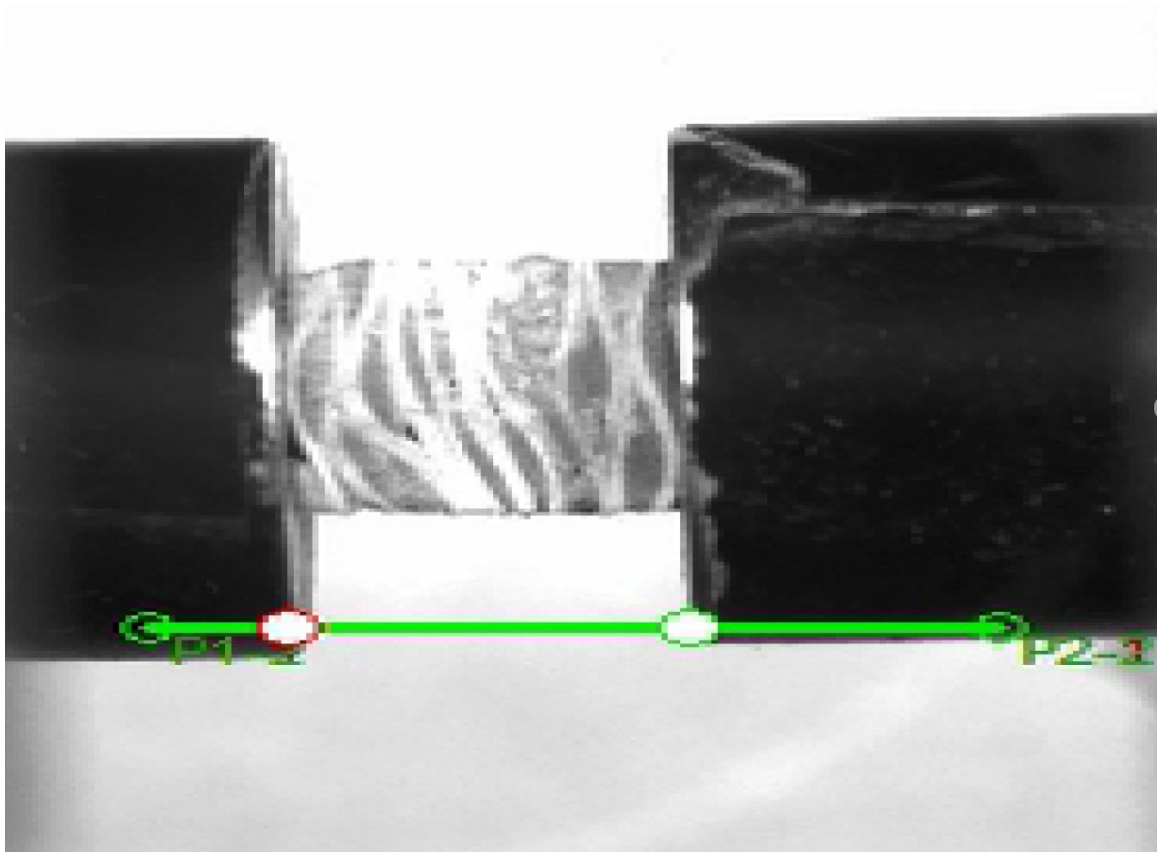

Figure 9: 1-D tracking for DIC analysis

RESULTS AND DISCUSSION

Level 1 Results

The Level 1 samples were tested within the high strain rate of ~860/s to ~1850/s. Stress vs. strain curves were generated for all 9 samples. Figure 10 is an overlay of all the samples' stress vs. strain curves.
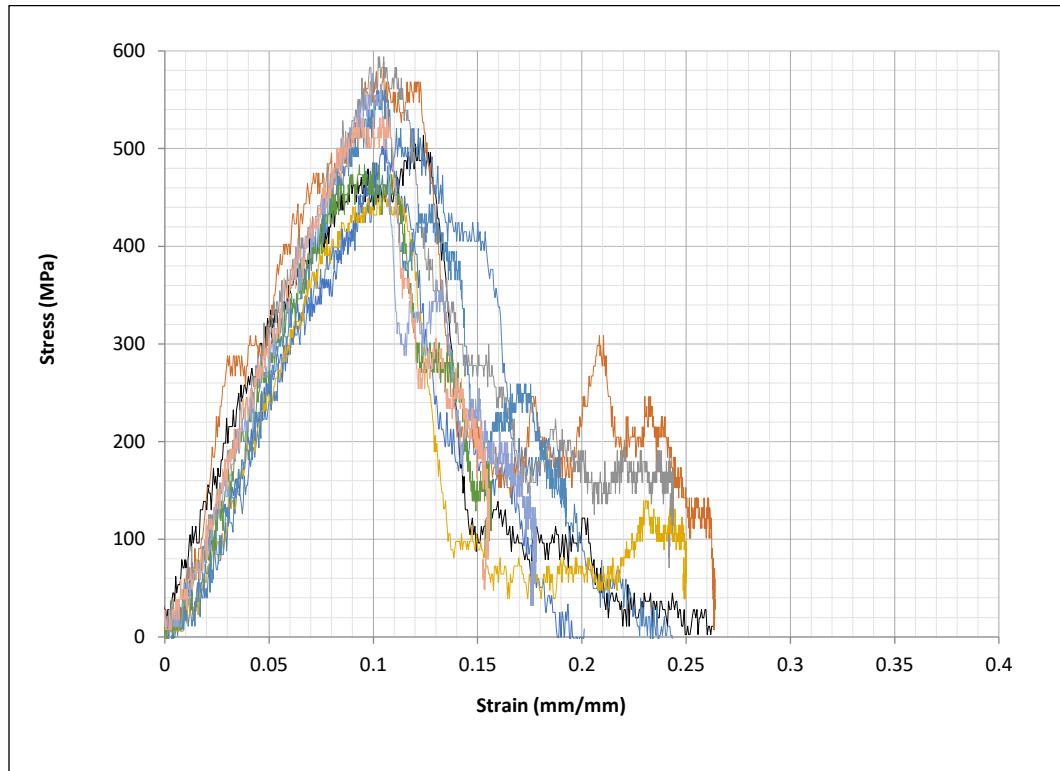

Figure 10: Level 1 Stress vs. Strain

The graph shows a variation in peak stress, ranging from 547-595 MPa. The strain at which peak stress occurred, however, hovered close to 11%. Despite the range in peak stresses, there was no correlation to strain-rate sensitivity within this tested range. The range of peak stress can thus be achieved at any strain-rate. Figure 11 is a comparison of stress between a sample tested at 1300/s, at the high end of the strain rate range, versus a sample tested at 963/s at the low end. Both achieved a peak stress of approximately 560 MPa, on the higher end of the peak stress spectrum. Figure 12 compares a sample tested at 1625/s at the high end of the strain rate range, to one tested at 908/s at the low end; both achieved a peak stress of about 500 MPa which is at the low end of the peak stress spectrum. There is a couple of possible explanations as to why strain-rate sensitivity could not be seen. A failure mode may have occurred before strain-rate sensitivity

could be noted, or the material truly had no strain-rate sensitivity within the strain-rates tested. To justify the range of peak stresses without strain rate sensitivity, the observation of composites must be made. Many composites, especially DuroProtect, are nonhomogeneous. Nonhomogenous materials greatly depend on its sole components within the material. The fiber layers may have been thicker in some samples compared to others. Also, when the samples were cut, delamination at the raw edges may have occurred, causing premature failure. Rabbi et al.'s previous study on various laminated woven and auxetic composites of Kevlar with an epoxy matrix concluded that poor interlaminar shear strength attributes to edge failure of their samples. This is due to the lack of a consistent bond of epoxy between layers [15].
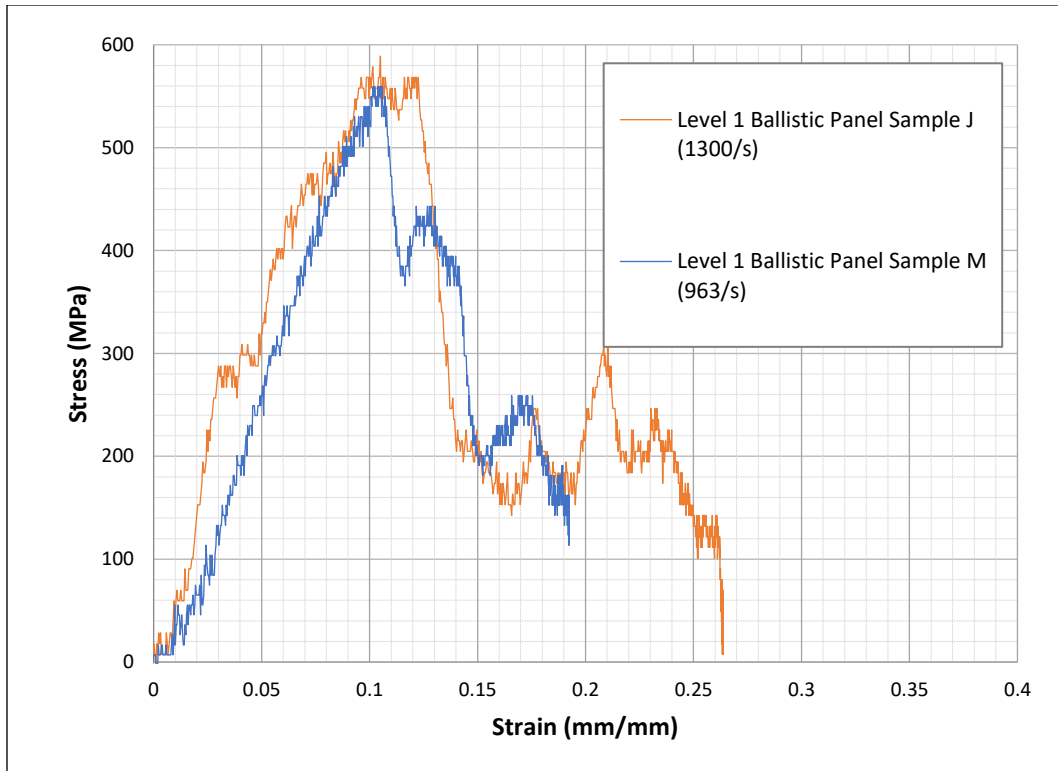

Figure 11: Level 1 strain-rate comparison of stress vs. strain curves for higher ultimate stress
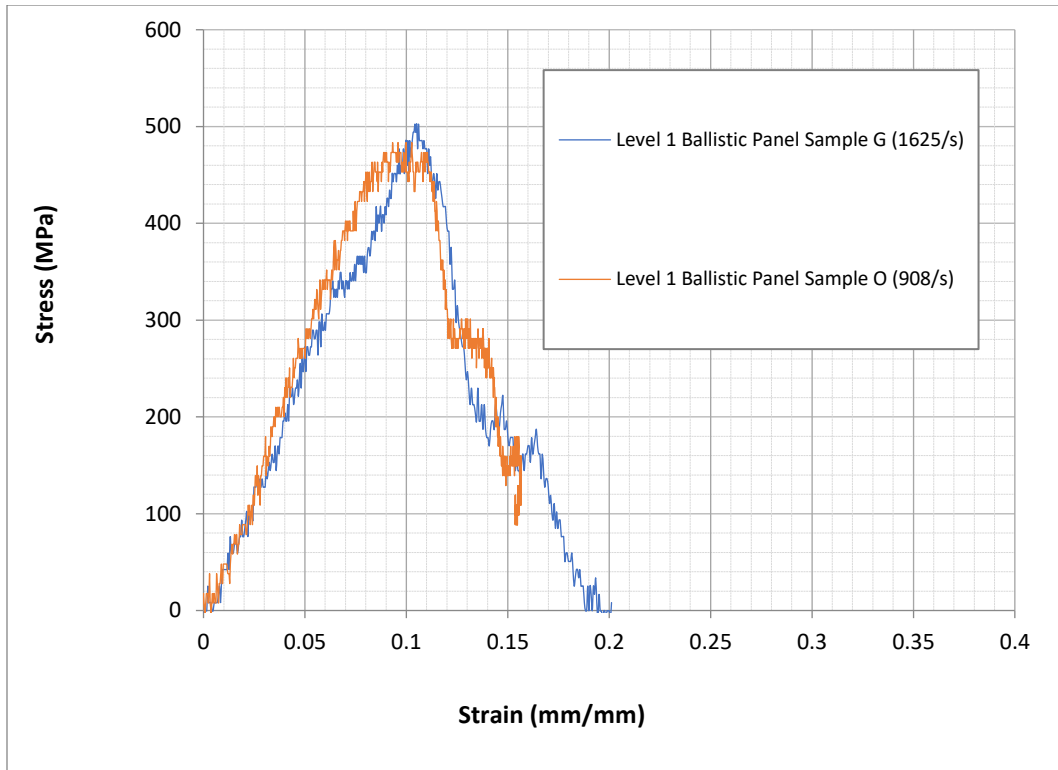
Figure 12: Level 1 strain-rate comparison of stress vs. strain curves for lower ultimate stress

Level 2 Results

The strain rate range for the nine Level 2 samples was between ~1375/s to ~2050/s; again, these are typically high strain rates simulating a sudden impact. Figure 13 shows an overlay of all the stress vs. strain curves for the Level 2 samples. A range of peak stresses was achieved between 274-395 MPa at a compressive deformation of about 17.4%.
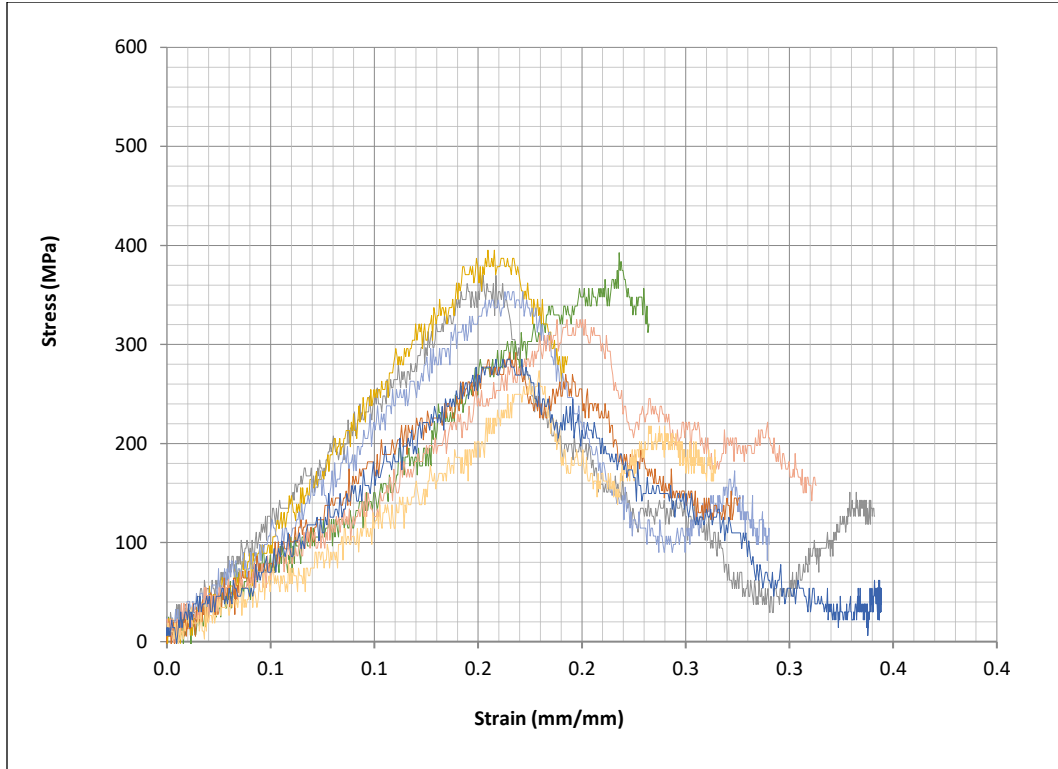
Figure 13: Level 2 Stress vs. Strain

A similar trend is seen in Level 2 as was in Level 1. There is no correlation between the peak stresses and their strain rates. There is a mix of various strain rates relating to various peak stresses, thus any strain rate within its range can achieve any peak stress within its range. Figure 14 is a comparison between two similar strain-rates with peak stresses at opposite ends of its range. The sample achieving a peak stress of approximately 395 MPa was impacted at a strain rate of 1600/s. Another sample achieved a peak stress of 290 MPa at a similar strain rate of 1650/s. Again, like the Level 1 samples, variations in peak stresses is attributed to the nonhomogeneous makeup of the composite. Matrix inconsistencies could have interfered with the overall dynamic properties [15].

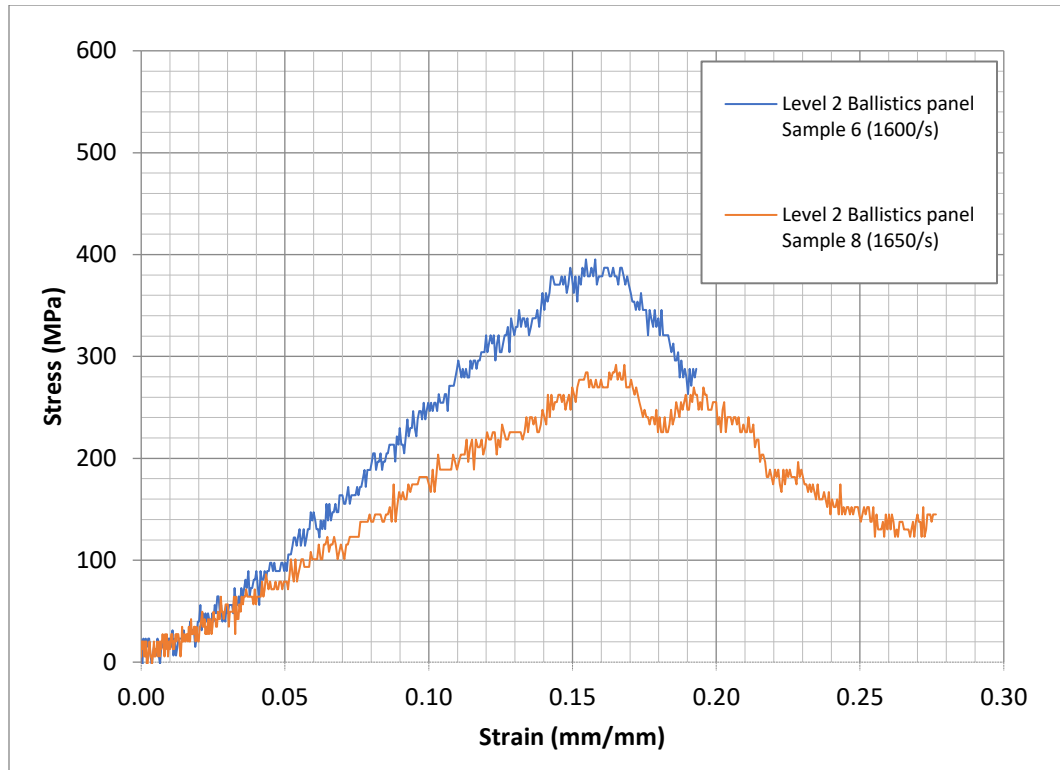Figure 14: Comparison of similar strain-rates achieving different peak stresses

Comparison

Along with analyzing the two thicknesses individually, a comparison between the two were also made. Since no attributions to strain-rate sensitivity was found for either thicknesses, a valid comparison between their dynamic properties could be made. The dynamic property ranges for both Level 1 and Level 2 are listed in Table 1.

Table 1: Dynamic Properties of DuroProtect Level 1 and Level 2

	Level 1 DuroProtect	Level 2 DuroProtect
Strain-Rate (/s)	863-1850	1375-2050
Ultimate Compressive Strength (MPa)	547-595	274-395
Maximum Specific Energy (kJ/kg)	21-36	25-44
Damage Initiation Energy per unit mass (kJ/kg)	11.6-20.0	13.6-23.8
Damage Propagation Energy per unit mass (kJ/kg)	7.3-19.7	11.8-22.4
Strain to Max Load (mm/mm)	0.093-0.124	0.131-0.218

Figure 15 is a graphical representation of the comparison between the ultimate compressive strengths, or peak stresses for Level 1 and Level 2. Figure 16 is the strain at which the ultimate compressive strengths were achieved. Level 1 was found to achieve significantly greater ultimate compressive strengths at 10% compression than Level 2 at 17% compression. The ultimate compressive strength of Level 1 was 1.38-2.17 times greater than that of Level 2. The number of layers that contribute to the thickness may have been the affecting factor in ultimate compressive strength. With fewer layers in the Level 1 than in Level 2, the entire thickness of the samples had most likely reached its maximum compression thickness and allowed stress to greatly build before failure. Another possibility may be contributed to the manufacturing process. With a larger thickness in the Level 2, there is a higher possibility and risk for greater amounts of defects within the matrix of the composite. These defect locations can cause the material to fail prematurely, preventing the material from incurring higher stresses [15].
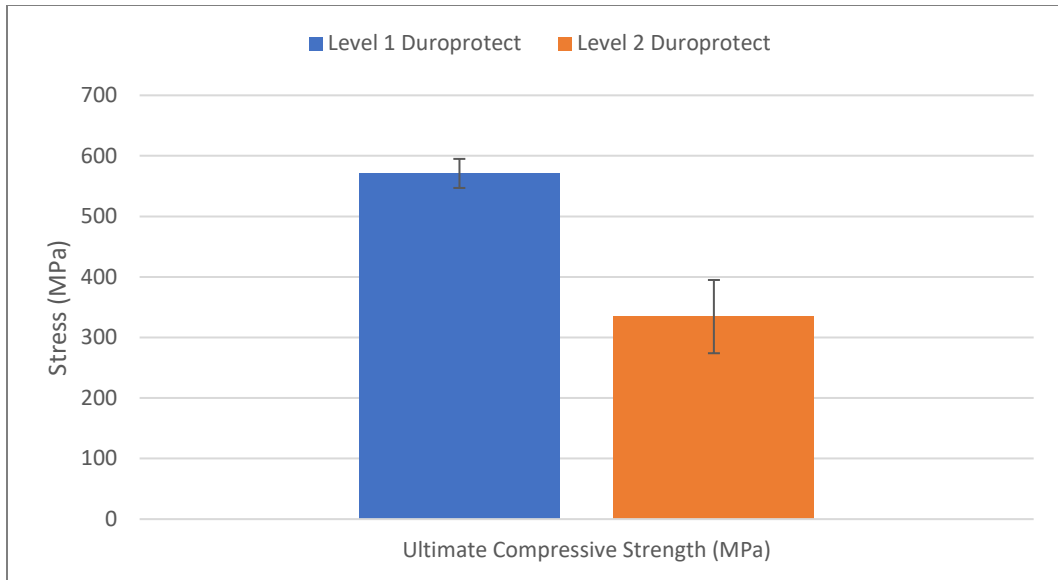
Figure 15: Ultimate compressive strength for Level 1 and Level 2

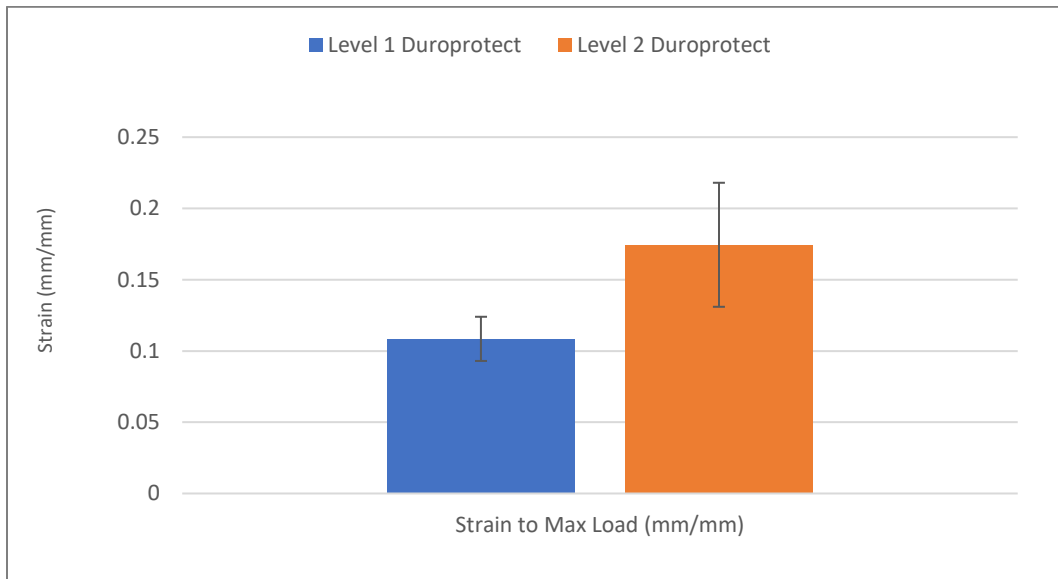Figure 16: Strain to max load values for Level 1 and Level 2

Although Level 1 samples had achieved higher peak stresses, Level 2 was found to absorb more energy from the impact. Overall maximum energy absorbed by the material is calculated as the area under the stress vs. strain curve. The energy absorption can be categorized into two types: damage initiation energy and damage propagation energy. Damage initiation

energy is the amount of energy absorbed before failure. This value is important, as it quantifies how much energy is needed in order to damage the sample. The more energy it can absorb before failure, the more load it can handle, or the more time is allowed to move to a safer area before catastrophic damage occurs. Damage propagation energy is the amount of energy absorbed after failure. Although the material has ultimately failed, the cracked pieces of the material are still compressing together and absorbing some energy from the impact. The material system, however, cannot absorb as nearly as much energy as it could before failure. Figure 17 is a mock stress vs. strain curve with how the energy absorption is visualized under the curve.
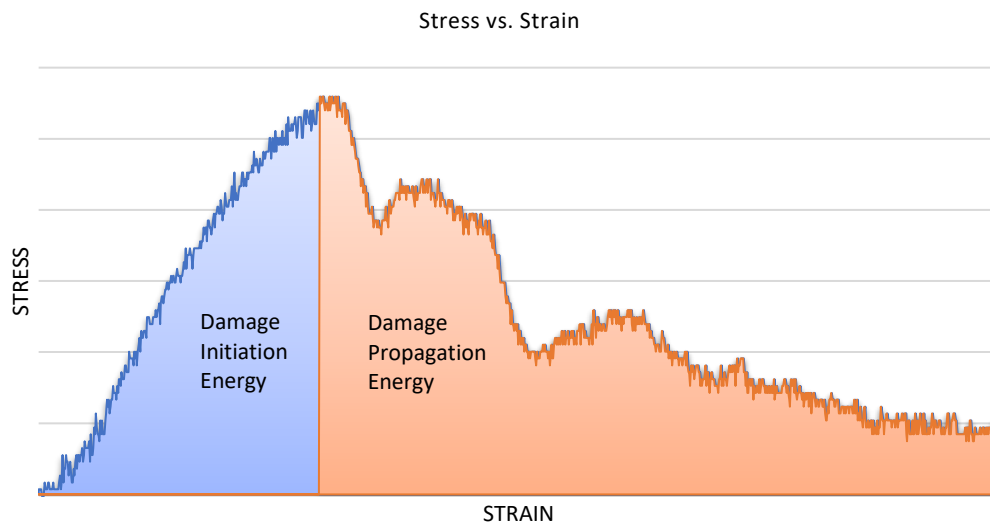

Figure 17: Energy absorption, visualized

The point where damage initiation ends and damage propagation occurs is the failure point. This point also represents the peak stress, or ultimate compressive strength. Figure 18 is a visual representation of the various energy values seen in the experiment. As evident, Level 2 was able to absorb more energy at about 1.44-2.09 times greater than Level 1. Level 2 had more material through the thickness to absorb the energy from impact. The absorbed energy is dissipated through fracture surfaces; Level 2 had a greater thickness, thus allowing for more

fracture surfaces to propagate. Saravanakumar et al. conducted a study on indentation of glass fiber/epoxy laminates that agreed with this conclusion on the effects of sample thickness [16].
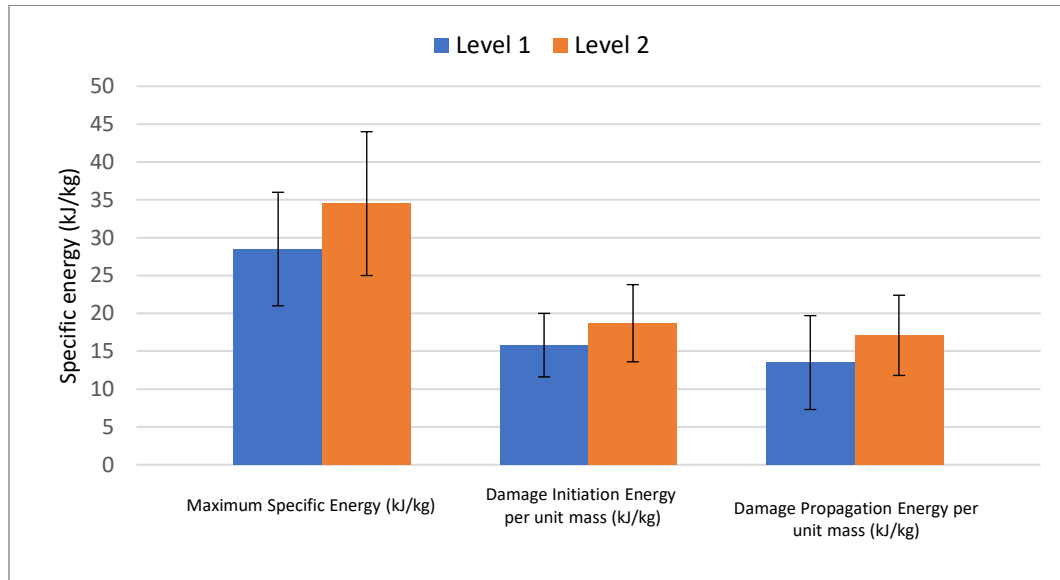

Figure 18: Energy values for Level 1 and Level 2

The major differences in the two configurations of Level 1 and Level 2 were their respective thicknesses and material ratios. Figure 19 shows a stress vs. strain curve for a sample found at the median of curves for each Level 1 and Level 2. Stiffness can be seen as the initial slope of the linear portion of the stress vs. strain curve. The stiffness indicates how likely a material is to deflect to an amount of load. Toughness is also related to stiffness. Toughness is favorable to a slope that is ductile yet strong, meaning a slope close to 1 is desirable. As seen in Figure 19, the Level 1 samples exhibited very stiff properties, while the Level 2 panels showed a more gradual curve, allowing more deflection. This difference is most likely attributed to the overall thicknesses of the samples. H. Wada et al. conducted a study that explored how the thickness of a sample had an effect on its fracture toughness. Results showed a correlation between high fracture toughness with a thinner thickness on their samples of polymethyl methacrylate. Wada concluded this phenomenon was due to a relaxation around the initial crack propagation transverse to thickness [17].
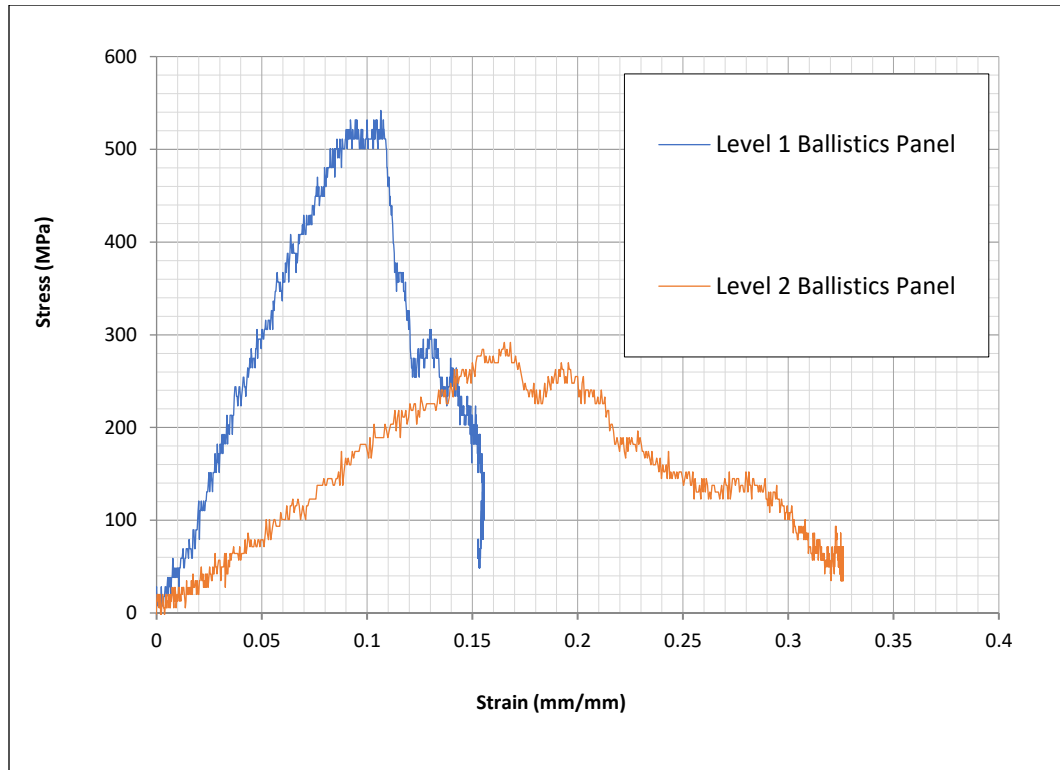
27

Figure 19: Stress vs. Strain comparison between samples from Level 1 and Level 2

DIC Analysis Results

DIC Analysis was used to confirm results from strain gage data. Data was confirmed to be reliable with 1-D tracking. Figure 20 shows the comparison of the high-speed video stills of the sample to different points of strain on the stress vs. strain curve of a Level 2 sample. The compressive wave began at 0 µs, where the sample has not yet been loaded. As the sample was compressed, no visible defects were seen up until about 130 µs. At this point was the first sign of failure, and damage propagation began at the middle of the thickness of the sample. With the compressive failure, peak stress was recorded to be 270 MPa. The stills at 230 µs and 272 µs depicted the debris after compressive failure, as the sample was still being compressed. The rising stress after failure was due to the fragments still being compressed. The fragments no longer had the same strength as the undamaged sample. Figure 21 compares the strain over time for both the conventional elastic wave theory analysis with DIC analysis. The two curves generally had matching slopes at the linear portion, confirming the overall data was sufficiently accurate. The small difference in the

beginning of the test was due to the DIC analysis not being able to identify toeing, or preloading of the sample.
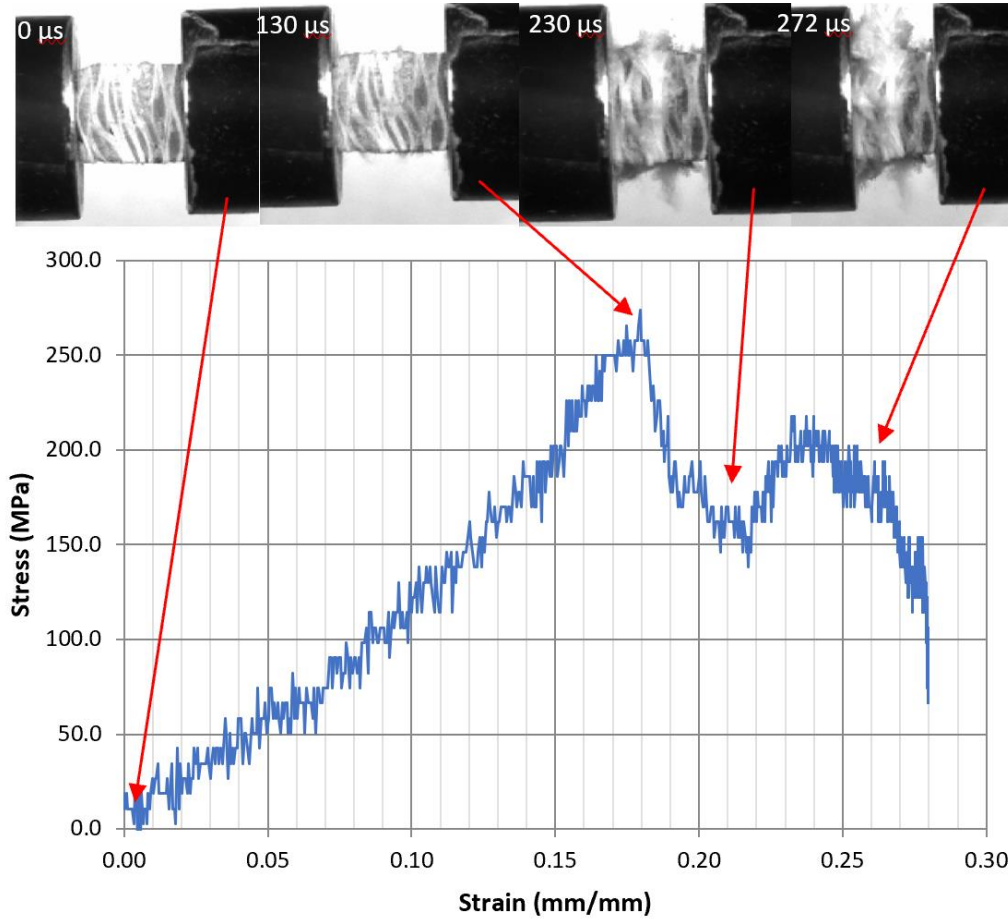

Figure 20: Side-by-side comparison of video footage and stress vs. strain for a Level 2 sample
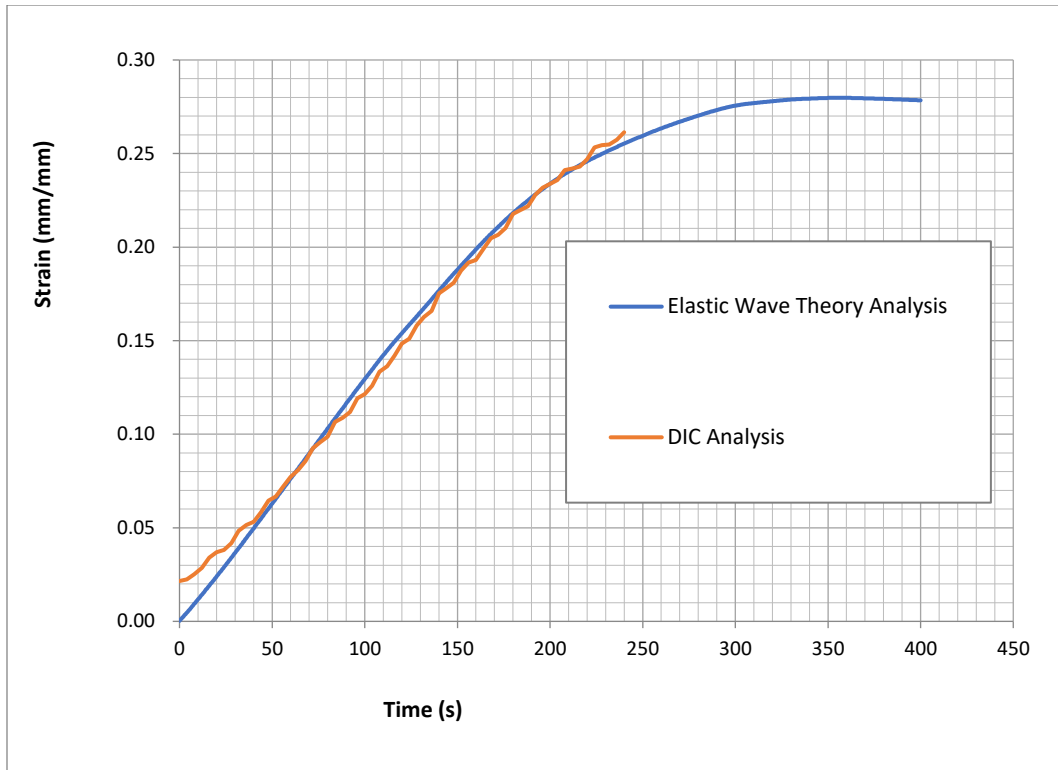
Figure 21: Strain vs. time comparison of conventional analysis with DIC analysis

CONCLUSION

Using the SHPB tests, the stress-strain curves were obtained for DuroProtect various high strain-rates from 800 /sec to 2000 /s. In general most composites exhibit an increase in compressive strength under high strain-rate loading as compared to quasistatic loading. The present results showed no strain-rate sensitivity within the strain-rates tested for either Level 1 or Level 2, disproving the original hypothesis. The variations in the dynamic properties can be attributed to inhomogeneity, such as fiber/matrix interfaces, layering, and dissimilar materials. Level 1 had approximately 1.38 – 2.17 times higher ultimate strengths than the Level 2; however, it had 1.44-2.09 times lower specific energy absorbed than Level 2. This may have been due to the smaller thickness in Level 1 compared to Level 2 or the inconsistency in the material manufacturing method.

With no conclusive evidence for a strain-rate effect within the ranges tested, there was also no evidence for strain hardening as other fiber composite materials have exhibited. The material seemed to have the same dynamic properties at any level of high strain-rate compressive loading. Comparing across different levels of DuroProtect, however, did show variances in dynamic mechanical properties.

It is possible to conduct further studies with DuroProtect to investigate other strain-rate sensitive behaviors. The present study did not obtain data under quasistatic loading conditions. A comparison with quasistatic testing can be performed, in which may reveal a prominent strain-rate and strain hardening effects between low and high strain-rates. Computational modelling can also be performed to identify the failure mechanism for Level 1 and Level 2 composites. Low velocity impact testing can also be performed to understand the material response in different loading conditions. Weathered samples can also simulate how the DuroProtect panels' dynamic properties may have changed after exposure to outdoor conditions. These several tests and many others can be performed to create a full profile of the material DuroProtect.

REFERENCES

[1] J. R. A. R. Bunsell, Fundamentals of Fibre Reinforced Composite Materials, Bristol: Institute of Physics Publishing, 2005.

[2] Rochling, "Ballistic Protection Materials: Composites," 2015. [Online]. [Accessed 20 March 2020].

[3] M. F. Omar, H. M. Akil, Z. A. Ahmad, A. Mazuki and T. Yokoyama, "Dynamic Properties of Pultruded Natural Fibre Reinforced Composites Using Split Hopkinson Pressure Bar Technique," *Materials & Design,* vol. 31, no. 9, pp. 4209-4218, 2010.

[4] M. Guden, U. Yildirim and I. W. Hall, "Effect of Strain Rate on the Compression Behavior of a Woven Glass Fiber/SC-15 Composite," *Elsevier Polymer Testing,* p. 719–725, 2004.

[5] N. K. Naik and et. al., "High Strain Rate Tensile Behavior of Woven Fabric E-glass/Wpoxy Composite," *Polymer Testing,* vol. 29, no. 1, pp. 14-22, 2010.

[6] W. Kim and et. al., "High Strain-Rate Behavior of Natural Fiber-Reinforced Polymer Composites," *Journal of Composite Materials,* vol. 46, no. 9, pp. 1051-1065, 2012.

[7] W. Chen and B. Song, Split Hopkinson (Kolsky) Bar: Design, Testing, and Applications, London: Springer, 2011.

[8] I. Živković, C. Fragassa, A. Pavlović and T. Brugo, "Influence of Moisture Absorption on the Impact Properties of Flax, Basalt, and Hybrid Flax/Basalt Fiber Reinforced Green Composites," *Composites Part B: Engineering,* vol. 111, pp. 148-164, 2017.

[9] A. P. C. Barbosa, A. P. P. Fulco, E. S. S. Guerra, F. K. Arakaki, M. Tosatto, M. C. B. Costa and J. D. D. Melo, "Accelerated Aging Effects on Carbon Fiber/Epoxy Composites," *Composites,* vol. 110, pp. 298-306, 2016.

[10] J. M. Gere and B. J. Goodno, Mechanics of Materials, Eighth Edition, Stamford: Cengage Learning, 2013.

[11] H. D. Young, University Physics, Reading: Addison-Wesley Publishing Company, 1992.

[12] W. Chen, B. Zhang and M. J. Forrestal, "A Split Hopkinson Bar Technique for Low-Impedance Materials," *Experimental Mechanics,* vol. 39, no. 2, pp. 81-85, 1999.

[13] D. J. Frew, M. J. Forrestal and W. Chen, "Pulse Shaping Techniques for Testing Brittle Materials With a Split Hopkinson Pressure Bar," *Experimental Mechanics,* vol. 42, no. 1, pp. 93-106, 2002.

[14] C. Siviour and J. Jordan, "High Strain Rate Mechanics of Polymers: A Review," *Journal of Dynamic Behavior of Materials,* vol. 2, no. 10, 2016.

[15] M. F. Rabbi, V. Chalivendra and Y. Kim, "Dynamic Constitutive Response of Novel Auxetic Kevlar®/Epoxy Composites," *Composite Structures,* vol. 195, pp. 1-13, 2018.

[16] K. Saravanakumar, B. S. Lakshminarayanan and V. Arumugam, "Effect of Thickness and Denting Behavior of Glass/Epoxy Laminates Subjected to Quasi-Static Indentation (QSI) Loading Under Acoustic Emission Monitoring," *Journal of Nondestructive Evaluation,* vol. 37, no. 3, 2018.

[17] H. Wada, M. Seika, T. Kennedy, C. Calder and K. Murase, "Investigation of loading rate and plate thickness effects on dynamic fracture toughness of PMMA," *Engineering Fracture Mechanics,* vol. 54, no. 6, pp. 805-811, 1996.